International Journal of Nanoelectronics and Materials
IJNeaM
ISSN 1985-5761 | E-ISSN 2232-1535

Effect of TiO_2 thickness on power conversion efficiency in co-sensitized dye-sensitized solar cells

Emy Zairah Ahmad [a] *, Muhammad Safuan Md Ali [a], Muhammad Idzdihar Idris [b] and Mohd Shahneel Saharudin [c]

[a]*Faculty of Electrical and Technology Engineering, Universiti Teknikal Malaysia Melaka (UTeM), 76100, Melaka, Malaysia*
[b]*Faculty of Electronic & Computer Technology and Engineering, Universiti Teknikal Malaysia Melaka (UTeM), 76100, Melaka, Malaysia*
[c]*Robert Gordon University, School of Engineering, Garthdee Road, AB10 7QB, Aberdeen, United Kingdom*
** Corresponding author. Tel.: +6-018-575-1042; e-mail: emyzairah@utem.edu.my*

Received 16 May 2025, Revised 20 November 2025, Accepted 18 December 2025

ABSTRACT

This study investigates the co-sensitization of natural dyes with synthetic dye N719 in dye-sensitized solar cells (DSSCs). Natural dyes from Spinacia oleracea (green spinach) and Plumeria rubra (frangipani) were extracted and analyzed via UV-Visible spectroscopy to assess their light absorption capabilities. Co-sensitization was carried out by blending these extracts with N719, aiming to broaden the absorption spectrum and improve overall efficiency. The impact of titanium dioxide (TiO_2) photoanode thickness (55,000 nm and 110,000 nm) and different substrates (indium tin oxide and fluorine-doped tine oxide) on the power conversion efficiency (PCE) was systematically studied under controlled fabrication conditions using 4 different cases (Case A, Case B, Case C, and Case D). Among the four dye combinations tested, the N719-frangipani co-sensitized DSSC fabricated on FTO glass with a 110,000 nm TiO_2 layer demonstrated the highest PCE of 0.0324%. In contrast, the lowest performance (0.000014%) was observed in the cell sensitized with a spinach–frangipani blend on ITO. UV-Visible spectral analysis confirmed broader light absorption for co-sensitized dyes, while I–V characterization revealed enhanced charge transport in thicker photoanodes and FTO-based cells. These findings demonstrate the potential of co-sensitization using natural dyes to partially replace synthetic dyes, offering a cost-effective and environmentally friendly approach to DSSC fabrication.

Keywords: *Dye-sensitized solar cell, Co-sensitization, Natural dyes, Synthetic dye (N719), Power conversion efficiency*

1. INTRODUCTION

The increasing demand for sustainable energy solutions has encouraged the exploration of solar technology, leading to advancements in various innovative applications. This has paved the way for emerging technology known as Dye-Sensitized Solar Cells (DSSCs) which are flexible and cost-effective alternative to conventional Silicon-based photovoltaic [1]. The first remarkable DSSC was fabricated in 1991 by B. O'Regan and M. Gratzel using TiO_2 and Ru dye complexes with power conversion efficiency of 7.12% [2]. In comparison to conventional Si-based photovoltaics, DSSCs offer simpler fabrication, economical and eco-friendly, hence attracted researchers the most.

The fundamental component of a DSSC contains the photosensitizer, a vital element that absorbs sunlight. Photosensitizers can be extracted from natural sources like plant pigments or fruit dyes, or they can be manmade substances [3]. In general, dye photosensitizers can be categorized into two categories: synthetic and natural sensitizers, as depicted in Figure 1. Synthetic dyes have enhanced efficiency and stability within cells, hence presenting considerable promises for commercial utilization [4]. However, the manufacturing of dyes containing Ruthenium is expensive and require complex synthesis methods that have negative environmental effects and pose health hazards due to their poisonous nature [5]. The use of natural dyes as photosensitizers has emerged as a prominent area of investigation in contemporary study. The research is motivated not only by the need for enhanced performance but also by prioritizing sustainability and environmental concerns associated with the employed materials.

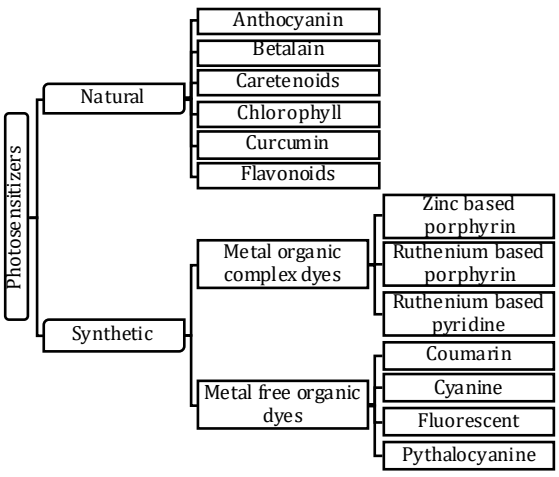

Figure 1. Classification of dye used as photosensitizers

The effective range for photo absorption in natural dyes is highly influenced by the type of plant's pigmentation [6]. Among the pigments that show promising performance as natural photosensitizers are anthocyanin, betalain, carotenoid, chlorophyll, curcumin, and flavonoid. The most abundant and well-known pigment is anthocyanin despite its high sensitivity to changes in pH. Their colors may vary depending on the acidity or alkalinity of the environments [7–9]. For instance, in acidic conditions, they will appear red, while in more alkaline environments, they tend to be blue or purple. Similar research was carried out under both alkaline and acidic dye solutions using Malabar spinach [10]. The maximum absorption was observed at a wavelength of 540 nm under acidic condition outperforms the alkaline solution.

Among the naturally occurring pigments, anthocyanins seem to be a highly suitable substitute for utilization in DSSCs. Alternatively, the utilization of natural dyes extracted from Chrysanthemum flowers was examined. The researchers extracted dyes from flowers of three different colors: violet, green, and blue, which are rich in anthocyanin. They found that the dye extracted from Chrysanthemum violet produced the highest conversion efficiency (1.348%) compared to green and blue cells [11]. On the other hand, Shah *et al.* [12] focuses on the use of beetroot and curcumin extracts as photosensitizers. The study discovered that co-sensitizing DSSCs with a combination of betalain extract from beets and curcumin extract from turmeric increased cell efficiency [13, 14]. This was due to a larger absorption spectrum and more light absorption as compared to utilizing a single dye. The optimized dye combination has a maximum cell efficiency of 0.649%. Likewise, Dang Quang *et al.* [15] explored the co-sensitization method using both synthetic and natural dyes. The results revealed that the best performance was achieved under different concentration of dyes.

Based on the literature, very limited studies were observed on co-sensitization using both natural and synthetic dyes. Natural dyes tend to have restricted light absorbance as well as less stability. Co-sensitization with synthetic dyes like N719 presents a strategic alternative to widen the range of light absorbance and the efficiency of charge transfer. Intermixing of natural dyes like Spinacia oleracea and Plumeria rubra with N719 in this paper is intended to find synergistic properties that ensure the enhancement of the overall efficiency performance of DSSCs.

1.1. Fundamental Principles of DSSC Operation

The fundamental component of a DSSC contains the photosensitizer, a vital element that absorbs sunlight. Photosensitizers can be extracted from natural sources like plant pigments or fruit dyes, or they can be manmade substances. DSSCs employ dyes to capture photons and transform them into energized electrons [16]. The DSSC consists of multiple layers, namely the front transparent conducting electrode (TCE), the dye-sensitized semiconductor layer, the electrolyte, and the rear counter electrode (CE). Figure 2 illustrates the key mechanisms that are involved in the operation of DSSC. The front TCE allows sunlight to pass through while also transmitting electrons. The dye-sensitized semiconductor layer (working electrode) absorbs sunlight, causing electrons to be excited and injected into the semiconductor. The working electrode is coated in a layer of titanium dioxide, which furthers sensitized using selected dyes. This technique results in increased porosity, hence enhancing the penetration of sunlight into the semiconductor layer. The back CE promotes redox couple reduction and completes the electrical circuit.

To ensure the efficacy of DSSCs, it is important to ensure the sensitizer used offers a wide spectrum of absorption capabilities, covering both the visible and near-infrared regions [17]. Hence, the determination of the energy gap relies on the analysis of the absorbance data inside the visible band (400–600 nm).

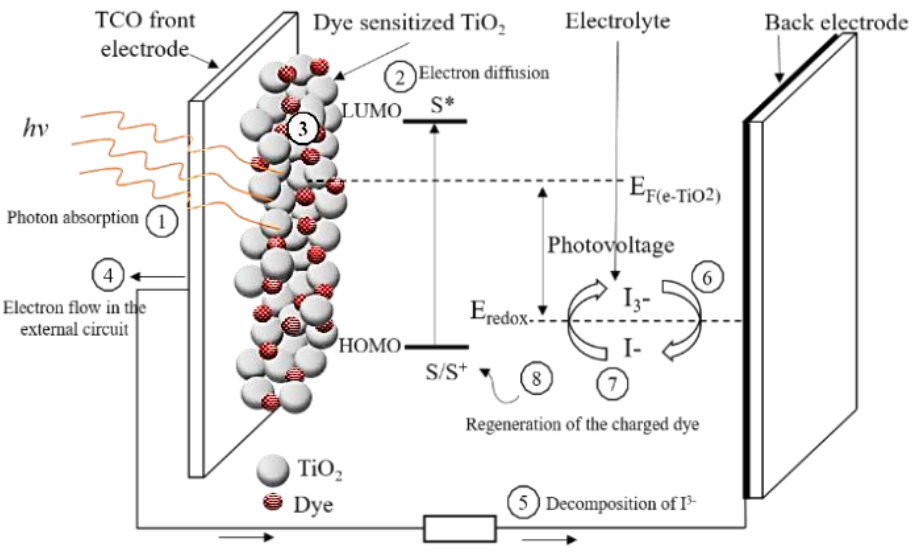

Figure 2. Schematic representation of elementary processes in DSSC

2. METHODOLOGY

The methodology of this study involves the experimental fabrication and characterization of dye-sensitized solar cells (DSSCs) using two types of natural dyes; Plumeria rubra (PR) and Spinacia oleracea (SO) along with synthetic dye (N719) combinations. Four case studies were conducted to investigate the effects of co-sensitization, TiO_2 thickness, and substrate type (ITO and FTO) on power conversion efficiency (PCE). Cases A, B, and C were fabricated using an ITO substrate with different dye combinations: Plumeria rubra (PR) + Spinacia oleracea (SO), N719 + SO, and N719 + PR, respectively. The best-performing combination among these was selected for further optimization in Case D using a more conductive FTO substrate. For each case, TiO_2 photoanodes were fabricated in two different thicknesses, approximately 55,000 nm and 110,000 nm. The UV-Vis spectroscopy was employed to analyze the light absorption behavior of each sample and current-voltage characterization was performed using Ossila solar simulator to evaluate the power conversion efficiency.

2.1. Ultraviolet-Visible Spectroscopy

The samples were tested for their capacity to absorb visible light using a UV-Vis spectroscopy. The UV-2450 equipment, having a wavelength range of 300 to 800 nm, was used to perform the investigation. The resultant spectrum, known as an absorption spectrum, reveals how much light the sample absorbs at each wavelength. The optical band gap of each sample was determined from the UV-Vis absorption spectrum using the following equations [18]:

$$(ahv)^n = A(hv - Eg) \tag{1}$$

$$E = \frac{1024}{\lambda} \tag{2}$$

$$\alpha = \frac{2.303A}{l} \tag{3}$$

The optical band gap for the absorption peak was calculated using Equation (1) whilst Equation (2) was used to determine the energy, E where λ is the absorption wavelength. In this equation, α represents the absorption coefficient of the material, which indicates how strongly the material absorbs light and is typically expressed in units such as cm^{-1}. The term h is Planck's constant, while ν is the frequency of the incident photon. The constant A is a material-dependent proportionality constant related to the probability of electronic transitions. The parameter E_g refers to the optical band gap energy, which is the minimum energy required to excite an electron. Further, the absorption coefficient, α was calculated using Equation (3), where A is the absorbance and l is the sample thickness.

2.2. Power Conversion Efficiency from Current-Voltage Characterization

The electrical characterization of DSSCs involves measurement of several parameters. Power conversion efficiency, PCE can be defined as the highest energy output obtained from a DSSC to the input sun energy (P_{in}) that is incident on the entire surface area of the solar cell, as represented by Equation (4) [19]:

$$PCE = \frac{\text{Fill factor } (FF) \times J_{SC} \times V_{OC}}{P_{in}} \times 100\% \tag{4}$$

In this equation, V_{oc} represents the open-circuit voltage in volts (V), J_{sc} represents the short-circuit current density in milliamperes per square centimetre ($mA \cdot cm^{-2}$), FF represents the fill factor, and P_{in} represents the power of the incident light.

3. EXPERIMENTAL PROCEDURES

This project involves fabricating and characterizing dye-sensitized solar cells (DSSCs) using co-sensitization between natural and synthetic dyes as sensitizers.

3.1. Dyes Preparation

The Spinacia oleracea (SO) and Plumeria Rubra (PR) were first cleaned in distilled water to get rid of any contaminants before being allowed to dry for 2 hours to get rid of moisture. Then, it was finely ground into green and red pastes and then soaked in ethanol solvent. Ethanol solvent is used because it has the potential to decrease the aggregation of dye molecules in comparison to water. The mixture of paste materials and ethanol ratio was 1 g : 10 ml. The extract was filtered and used as a raw sensitizer source.

3.2. Preparation of Electrolyte Solution

The electrolyte was prepared by combining 1.4 g of ethyl-methyl-imidazolium iodide (EMII), 0.6 g of 4-tert-butylpyridine (TBP), 0.13 g of lithium iodide (LiI), and 0.13 g of iodine in a vial. Then, 10 ml of acetonitrile was added, and the mixture was thoroughly stirred for 15 minutes using a hot plate to ensure the solution is well combined.

3.3. Preparation of Counter Electrode

The electrolyte solution was prepared by dissolving 10.36 mg Hexachloroplatinic acid hexahydrate in 10 ml Isopropyl Alcohol (IPA). The solution was mixed on hotplate at room temperature for 1 hour.

3.4. Preparation of Photoanode Layer

Position the Kapton film precisely as indicated, ensuring it covers only the designated 1 cm by 1 cm area as shown in Figure 3. Then, apply the TiO_2 paste onto the larger glass surface by holding it at a 45-degree angle, and carefully spread the paste toward the end of the glass, ensuring a smooth coating free of air bubbles. A single spread is applied, resulting in an approximate thickness of 55,000 nm, while two consecutive spreads produced a thickness of approximately 110,000 nm. Then, the photoanode thin film is baked in a furnace at 450 °C for 30 minutes to complete the process.

3.5. Preparation of Dye on Photoanode Layer

To prepare co-sensitized dye solutions, three combinations were used: Plumeria Rubra + Spinacia oleracea (50:50) (Case A), Spinacia oleracea + N719 (Case B), and Plumeria Rubra + N719 (Case C). The TiO_2-coated photoanodes were immersed in each dye solution and left overnight to ensure thorough adsorption, as shown in Figure 4 (a). After dyeing process, the photoanodes were rinsed with deionized water and dried in an oven at 100°C for 10 minutes.

3.6. Preparation of Counter Electrode Layer

The substrate is placed on the spin coater with the conductive side facing up. Then, 50 µL of platinum solution was dispensed and spun at 1500 rpm for 10 seconds. The counter electrode was then baked at 450°C for 30 minutes to ensure proper deposition and adhesion.

3.7. DSSC Fabrication

A DSSC structure is made up of a working electrode and a counter electrode sandwiched between two electrolytes. Three types of working electrodes were fabricated (Case A, Case B, Case C, and Case D), while the counter electrode is coated with Pt solution. As illustrated in Figure 5, the fabrication was achieved by combining the working electrode and the counter electrode in a sandwich form. Then, the completed DSSC is tested using a solar simulator (Keithley 2450) with simulated AM 1.5G light at 100 mW/cm^2.

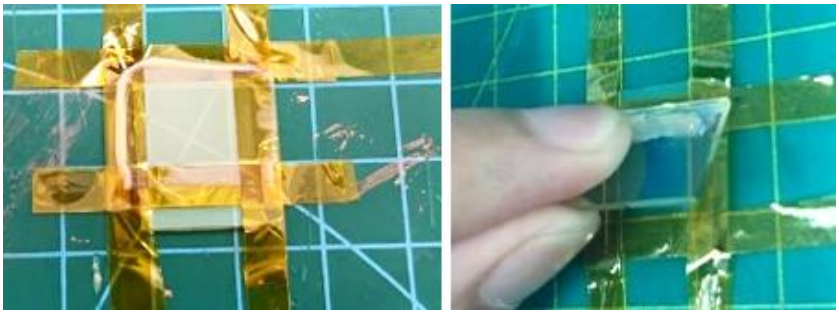

Figure 3. The TiO_2 paste was spread at 45-degree angle

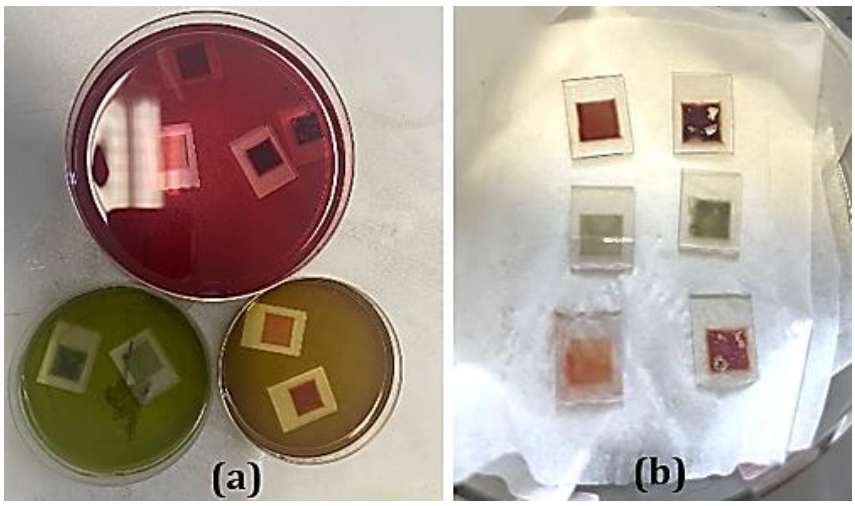

Figure 4. (a) Photoanodes immersed in dye solutions and (b) oven drying for 10 minutes

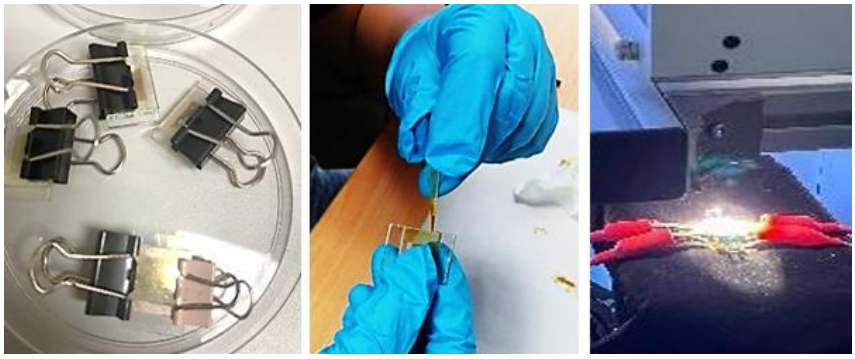

Figure 5. The device is ready for testing

4. RESULTS AND DISCUSSION

4.1. UV-Visible Analysis of Co-Sensitized Dyes with Single-Layer (55,000 nm) TiO_2 Photoanode

The UV-Vis absorption spectra shown in Figure 6 (a) demonstrates the absorbance patterns of four different co-sensitized dye attached to a single layer of TiO_2. The x-axis shows light wavelength in nanometers, while the y-axis represents absorbance in arbitrary units (a.u.).

The UV-Vis spectra for all four samples (1 layer of TiO_2) showed primary peaks between 391–393 nm and secondary peaks between 404–417 nm. The PR + SO (Case A) peaked at 392 nm and 416 nm, while SO + N917 (Case B) showed peaks at 391 nm and 404 nm. PR + N917 (Case C) exhibited strong absorption at 391 nm and 417 nm. The FTO-based sample (Case D) peaked at 393 nm and 409 nm. All spectra showed a gradual decline beyond 423 nm. These spectral variances are due to changes in the chemical structures of the dyes. Notably, as compared to natural dyes, the synthetic dye has a shorter absorption spectrum, implying higher selectivity in the wavelengths it can absorb. This property might be beneficial in solar cell applications, perhaps leading to improved efficiency.

Figure 6 (b) shows the Tauc Plot for four co-sensitized dye combinations. The optical bandgaps, determined using Tauc's method, were 2.76 eV for all PR-based samples and 2.81 eV for SO–N719 dye. The enhanced performance observed for the PR + N719 combination can be attributed to molecular structure compatibility between the two dyes. The carboxylic anchoring groups in both PR and N719 facilitate efficient binding to the TiO_2 surface, ensuring better electron injection into the conduction band. The complementary absorption spectra of PR (in the visible region) and N719 (extending toward the near-infrared region) allow for broader light harvesting. In addition, favorable band alignment between the LUMO levels of PR and N719 promotes sequential electron transfer, minimizing recombination losses. The strong π–π conjugation within N719 also enhances charge delocalization, improving electron mobility across the interface. Collectively, these synergistic interactions between molecular structure, band alignment, and electron transfer pathways explain the superior photovoltaic response of the PR + N719 system compared to the other dye pairings. This indicates that the Plumeria rubra contributes to narrowing the bandgap, enhancing electron mobility. A lower bandgap supports better solar performance by balancing light absorption and charge separation, while a higher bandgap may reduce the conductivity [20].

4.2. UV-Visible Analysis of Co-Sensitized Dyes with Double-Layer (110,000 nm) TiO_2 Photoanode

The UV-Vis absorption spectra shown in Figure 7 (a) demonstrates the absorbance patterns of four different co-sensitized dye attached to a double layer of TiO_2. The energy gap created by the 4 samples caused a significant drop in absorbance at short wavelengths. For the first spectrum, which consists of PR–SO (Case A), there is a significant peak at 355 nm and a smaller peak at 400. The second sample consists of SO–N917 (Case B) reveals a noticeable peak at 360 nm and a lesser peak at 406 nm. The third sample, PR–N917 (Case C) has a prominent peak at 355 nm, which is a combination of dyes from Plumeria Rubra and N719. The fourth sample, (Case D), has a large peak at 365 nm and a lesser peak at 404 nm. The variations in absorption spectra can be related to the dyes' unique chemical structures. A conjugated structure of double bonds in the spinach dye absorbs light in the blue and green portions of the spectrum [21]. The conjugated structure of frangipani dye absorbs light in the green and yellow parts of the spectrum. The synthetic dye has a complicated structure that allows it to absorb light at a broader variety of wavelengths. A dye-sensitized photoelectrode's absorption qualities are critical for its efficiency in converting light to energy. A dye that absorbs light at several wavelengths will be able to collect more energy from the sun [22]. However, in order to create electricity, the dye must be able to efficiently transport this energy to the TiO_2 semiconductor.

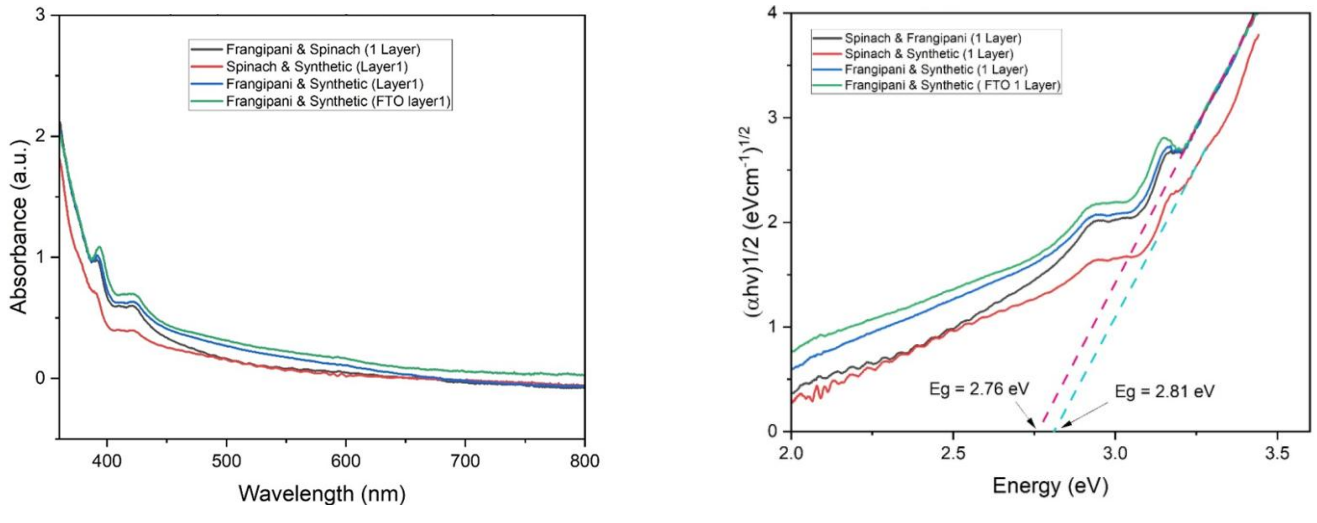

(a) (b)

Figure 6. (a) UV-Vis absorption spectra for a single layer of TiO_2 and (b) overall bandgap for a single layer of TiO_2

In the case of the double-layer TiO_2 structure, the increased film thickness enhances the light-harvesting capability by extending the optical path length, allowing more photons to be absorbed by the co-sensitized dyes. The observed peaks correspond to π–π electronic transitions within the conjugated dye molecules, signifying the excitation of electrons from the highest occupied molecular orbital (HOMO) to the lowest unoccupied molecular orbital (LUMO). The slight redshift observed in certain samples suggests improved electronic coupling between the dye and TiO_2, facilitating faster charge injection. The higher absorbance intensity in PR–N719 indicates efficient light utilization and better spectral overlap with the solar spectrum, which contributes to enhanced photocurrent generation. Thus, the spectral features reflect the synergistic effect of molecular structure compatibility and TiO_2 layer thickness on photon absorption and electron excitation efficiency.

The optical energy band gap (E_g) is derived using Equation (1). Regarding permitted indirect optical transitions, the value of n in the formula is equal to 2. The indirect bandgap was determined by plotting a graph between $(h\nu)^2$ and $(h\nu)$ in eV, as shown in Figure 7 (b). The band gap values for Case A, B, C and D are 3.17 eV, 3.05 eV, 3.37 eV, and 3.07 eV, respectively. Overall, these variations in band gap energy reflect the influence of dye molecular structure and TiO_2 layer configuration on the optical and electronic properties of the co-sensitized films.

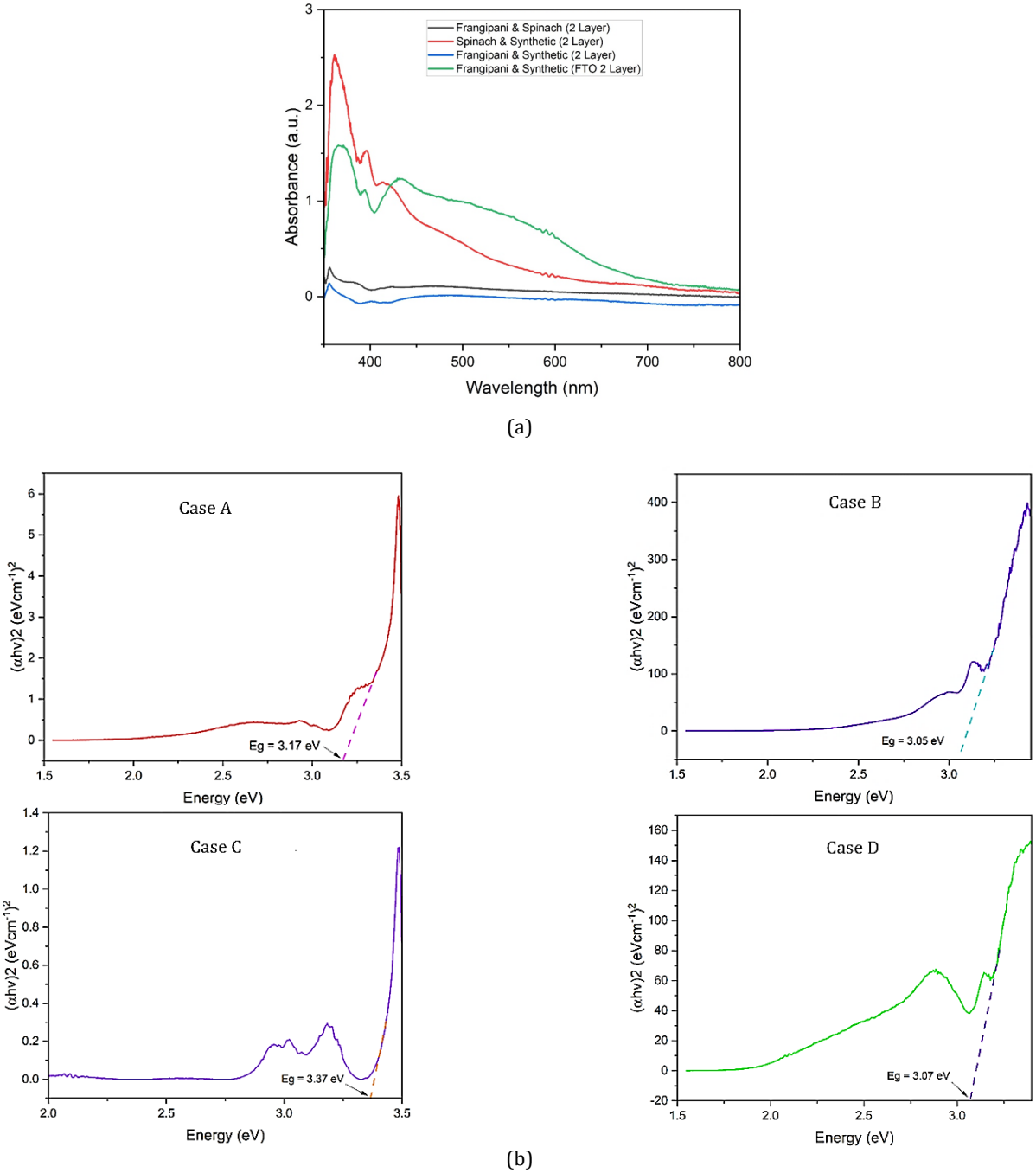

Figure 7. (a) Absorbance spectrum and (b) optical energy band gap

4.3. Current-Voltage Characteristics of Co-Sensitized DSSCs

The I-V characteristics of the fabricated DSSCs were analyzed based on different co-sensitizer combinations, TiO_2 layer thicknesses, and substrates. Among all samples, the highest efficiency of 0.0324% was achieved using frangipani co-sensitized with synthetic dye (N719) on an FTO glass substrate with a single TiO_2 layer (110,000 nm), attributed to its high V_{oc} (0.4 V) and J_{sc} (0.105010 mA/cm^2). In general, cells utilizing frangipani with N719 (Case C and D) outperformed those with spinach-based co-sensitizers (Case A and B), suggesting better charge transfer and dye compatibility. Additionally, thicker TiO_2 layers (110,000 nm) generally enhanced performance, except in Case A, where the single-layer configuration performed better. The results indicate that dye selection, TiO_2 layer optimization, and substrate type play significant roles in enhancing DSSC performance. The details of the I–V performance characteristics are illustrated in Figure 8.

4.4. Effect of TiO_2 Layer Thickness on Power Conversion Efficiency

Figure 9 illustrates the effect of TiO^2 layer thickness (55,000 nm and 110,000 nm) on the PCE of DSSCs with different co-sensitizer combinations. Across Cases A to C, an increase in TiO_2 thickness consistently enhanced PCE, indicating improved dye loading and better light harvesting. Case A, which used a fully natural dye (Plumeria rubra + green spinach), achieved the lowest PCE (0.000014% to 0.0045%). In contrast, Case C (N719 co-sensitized with Plumeria Rubra) recorded the highest PCE among ITO-based cells, increasing from 0.00154% to 0.0111%. Due to this promising performance, Case C was further characterized using an FTO substrate (Case D), resulting in the highest PCE of 0.0324%.

5. CONCLUSION

Based on the findings, several key conclusions can be drawn:

i. All samples with a single TiO_2 layer exhibited UV-Vis absorption peaks in the range of 391–393 nm (primary) and 404–417 nm (secondary), indicating effective light absorption in the visible spectrum. These absorption peaks correspond to π–π electronic transitions within the dye molecules, demonstrating efficient photon capture and electron excitation across the co-sensitized systems.

ii. The band gap values ranged from 3.05 eV to 3.37 eV, with Case C showing the widest gap and Case B the narrowest. The variation in band gap energies reflects the influence of molecular structure compatibility and the degree of electronic coupling between the dye and TiO_2, which in turn affects the charge transfer and recombination dynamics within the DSSC.

iii. Frangipani co-sensitized with synthetic dye (N719) consistently outperformed spinach-based combinations in terms of power conversion efficiency (PCE), highlighting better dye compatibility and charge transfer. This superior performance can be attributed to favorable band alignment between the highest occupied molecular orbital (HOMO)– and lowest unoccupied molecular orbital (LUMO) levels of both dyes and the TiO_2 conduction band, which promotes efficient electron injection and reduces energy losses due to recombination.

iv. Increasing TiO_2 thickness generally improved efficiency due to enhanced dye loading and light harvesting, except for Case A. However, excessive thickness may hinder electron transport and increase series resistance, suggesting that an optimal TiO_2 layer configuration is essential for achieving balanced optical absorption and charge mobility.

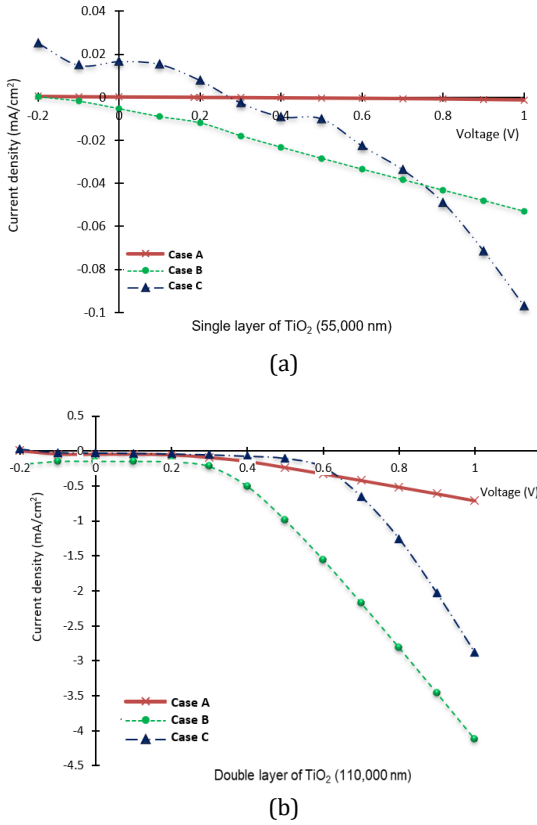

Figure 8. Current–voltage characteristics for (a) single layer and (b) double layer of TiO_2

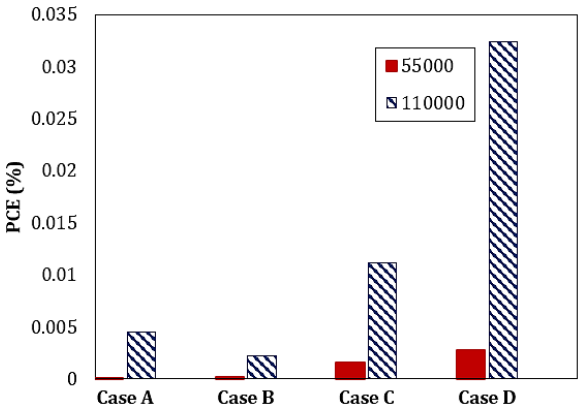

Figure 9. Power conversion efficiency for two different thickness of TiO_2 were observed

The best overall performance (PCE = 0.0324%) was achieved in Case D using frangipani + N719 on an FTO substrate, confirming the positive impact of substrate selection, dye pairing, and layer optimization on DSSC performance. Future work should explore additional dye combinations and surface modifications to further improve stability and overall conversion efficiency.

ACKNOWLEDGMENTS

The researchers express their appreciation to the Malaysian Ministry of Higher Education for providing financial support (PJP/2024/FTKE/PERINTIS/SA011), as well as to University Teknikal Malaysia Melaka (UTeM) for hosting the research and providing technical assistance.

REFERENCES

[1] U. Mahajan, K. Prajapat, M. Dhonde, K. Sahu, and P. M. Shirage, "Natural dyes for dye-sensitized solar cells (DSSCs): An overview of extraction, characterization and performance," *Nano-Structures & Nano-Objects*, vol. 37, p. 101111, 2024, doi: 10.1016/J.NANOSO. 2024.101111.

[2] M. K. Nazeeruddin, E. Baranoff, and M. Grätzel, "Dye-sensitized solar cells: A brief overview," *Solar Energy*, vol. 85, no. 6, pp. 1172–1178, 2011, doi: 10.1016/ j.solener.2011.01.018.

[3] K. Krishnakumar, A. Grover, and P. Kumar, "Performance of Multifarious Active Layer Materials in Organic Photovoltaic Cells: A Review," *International Journal of Nanoelectronics and Materials (IJNeaM)*, vol. 16, no. 4, pp. 933–946, 2024, doi: 10.58915/ijneam.v16i3.1380.

[4] G. Richhariya and A. Kumar, "Performance evaluation of mixed synthetic organic dye as sensitizer based dye sensitized solar cell," *Optical Materials*, vol. 111, p. 110658, 2021, doi: 10.1016/J.OPTMAT.2020. 110658.

[5] K. B. Erande *et al.*, "Extraction of natural dye (specifically anthocyanin) from pomegranate fruit source and their subsequent use in DSSC," *Materials Today: Proceedings*, vol. 43, pp. 2716–2720, 2021, doi: 10.1016/j.matpr.2020.06.357.

[6] S. Singh, I. C. Maurya, S. Sharma, S. P. S. Kushwaha, P. Srivastava, and L. Bahadur, "Application of new natural dyes extracted from Nasturtium flowers (Tropaeolum majus) as photosensitizer in dye-sensitized solar cells," *Optik*, vol. 243, 2021, doi: 10.1016/j.ijleo.2021.167331.

[7] C. Y. Chien and B. D. Hsu, "Optimization of the dye-sensitized solar cell with anthocyanin as photosensitizer," *Solar Energy*, vol. 9, pp. 203–211, 2013, doi: 10.1016/j.solener.2013.09.035.

[8] S. C. Ezike, C. N. Hyelnasinyi, M. A. Salawu, J. F. Wansah, A. N. Ossai, and N. N. Agu, "Synergestic effect of chlorophyll and anthocyanin Co-sensitizers in TiO_2-based dye-sensitized solar cells," *Surfaces and Interfaces*, vol. 22, p. 100882, 2021, doi: 10.1016/J.SURFIN.2020.100882.

[9] G. F. C. Mejica, Y. Unpaprom, D. Balakrishnan, N. Dussadee, S. Buochareon, and R. Ramaraj, "Anthocyanin pigment-based dye-sensitized solar cells with improved pH-dependent photovoltaic properties," *Sustainable Energy Technologies and Assessments*, vol. 51, p. 101971, 2022, doi: 10.1016/J.SETA.2022.101971.

[10] F. Kabir, M. M. H. Bhuiyan, M. S. Manir, M. S. Rahaman, M. A. Khan, and T. Ikegami, "Development of dye-sensitized solar cell based on combination of natural dyes extracted from Malabar spinach and red spinach," *Results in Physics*, vol. 14, p. 102474, 2019, doi: 10.1016/j.rinp.2019.102474.

[11] A. M. B. Leite, H. O. da Cunha, A. F. C. R. Rodrigues, R. Suresh Babu, and A. L. F. de Barros, "Construction and characterization of organic photovoltaic cells sensitized by Chrysanthemum based natural dye," *Spectrochimica Acta Part A: Molecular and Biomolecular Spectroscopy*, vol. 284, p. 121780, 2023, doi: 10.1016/j.saa.2022.121780.

[12] W. Shah, S. M. Faraz, S. Arshad, S. S. Haider, and M. H. Sayyad, "Co-Sensitized DSSC with Natural Dyes Extracted from Beetroot, Pomegranate and Cranberry," in *INTERACT 2023*, Basel Switzerland: MDPI, 2023, p. 13. doi: 10.3390/engproc2023 032013.

[13] W. Shah, S. M. Faraz, and Z. H. Awan, "Photovoltaic properties and impedance spectroscopy of dye sensitized solar cells co-sensitized by natural dyes," *Physica B: Condensed Matter*, vol. 654, 2023, doi: 10.1016/j.physb.2023.414716.

[14] S. Sowmya *et al.*, "Fabrication of natural dye-sensitized solar cells with bulk TiO_2 instead of nano-sized," *Optik*, vol. 242, p. 166205, 2021, doi: 10.1016/j.ijleo.2020.166205.

[15] L. N. Dang Quang, A. K. Kaliamurthy, and N. H. Hao, "Co-sensitization of metal based N719 and metal free D35 dyes: An effective strategy to improve the performance of DSSC," *Optical Materials*, vol. 111, p. 110589, 2021, doi: 10.1016/J.OPTMAT.2020. 110589.

[16] P. S. Saud *et al.*, "Dye-sensitized solar cells: Fundamentals, recent progress, and Optoelectrical properties improvement strategies," *Optical Materials*, vol. 150, p. 115242, 2024, doi: 10.1016/ J.OPTMAT.2024.115242.

[17] A. Agrawal, S. A. Siddiqui, A. Soni, and G. D. Sharma, "Advancements, frontiers and analysis of metal oxide semiconductor, dye, electrolyte and counter electrode of dye sensitized solar cell," *Solar Energy*, vol. 233, pp. 378–407, 2022, doi: 10.1016/ J.SOLENER.2022.01.027.

[18] X. Li *et al.*, "Determination of band gaps of self-assembled carbon nanotube films using Tauc/Davis-Mott model," *Applied Physics A*, vol. 97, no. 2, pp. 341–344, 2009, doi: 10.1007/s00339-009-5330-z.

[19] A. Kumar, A. Chaudhari, S. Kumar, S. Kushwaha, and S. Mandal, "Comparative study of natural and synthetic dyes in DSSCs: An experimental and computational approach," *Physica B: Condensed Matter*, vol. 685, p. 415978, 2024, doi: 10.1016/J.PHYSB.2024.415978.

[20] P. Panda, J. Kaur, R. Basu, A. K. Sharma, J. Madan, and R. Pandey, "Toward high-efficiency photovoltaics: MASnI3 and FASnI3 double absorber perovskite solar

cells with optimized conversion efficiency of 28%," *Physica B: Condensed Matter*, vol. 710, p. 417232, 2025, doi: 10.1016/J.PHYSB.2025.417232.

[21] A. S. Teja *et al.*, "Optimal processing methodology for futuristic natural dye-sensitized solar cells and novel applications," *Dyes and Pigments*, vol. 210, p. 110997, 2023, doi: 10.1016/J.DYEPIG.2022.110997.

[22] P. Sabarikirishwaran, Y. Unpaprom, and R. Ramaraj, "Effects of Natural Dye Solvent Extraction on the Efficiency of Dye-Sensitive Solar Cells from the Leaf Biomass of Sandoricum koetjape and Syzygium samarangense," *Waste and Biomass Valorization*, vol. 14, no. 10, pp. 3253–3263, 2023, doi: 10.1007/s12649-022-02030-2.